

The Ultra Luminous Infrared Galaxy MKN 231: New clues from *BeppoSAX* and *XMM-Newton*

V. Braito^{ab*}, R. Della Ceca^a, E. Piconcelli^{cd}, P. Severgnini^a, L. Bassani^c, M. Cappi^c, A. Franceschini^b, K. Iwasawa^e, G. Malaguti^c, P. Marziani^f, G.G.C. Palumbo^g, M. Persic^h, G. Risaliti^{ij} and M. Salvatiⁱ

^aINAF – Osservatorio Astronomico di Brera, Via Brera 28, 20154 Milano, Italy

^bDipartimento di Astronomia, Università di Padova, Vicolo Dell'Osservatorio 2, 35122 Padova, Italy

^cIASF – CNR, Sezione di Bologna, Via Gobetti 101, 40129 Bologna, Italy

^dXMM-SOC (VILSPA), ESA, 28080 Madrid, Spain

^eInstitute of Astronomy, University of Cambridge, Madingley Road Cambridge CB3 0HA, U.K.

^fINAF – Osservatorio Astronomico di Padova, Vicolo Dell'Osservatorio 5, 35122 Padova, Italy

^gDipartimento di Astronomia, Università di Bologna, Via Ranzani 1, 40127 Bologna, Italy

^hINAF – Osservatorio Astronomico di Trieste, Via Tiepolo 11, 34131 Trieste, Italy

ⁱINAF – Osservatorio Astrofisico di Arcetri, L.go E. Fermi 5, 50125 Firenze, Italy

^jHarvard-Smithsonian Center for Astrophysics, Cambridge, USA

We present *BeppoSAX* and *XMM-Newton* observations of MKN 231. These observations and in particular the *BeppoSAX* PDS data allowed us to unveil, for the first time, the highly absorbed ($N_H \sim 2 \times 10^{24} \text{ cm}^{-2}$) AGN component. We find that: a) the AGN powering MKN231 has an intrinsic 2-10 keV luminosity of $1_{-0.5}^{+1} \times 10^{44}$ erg/s; b) the strong starburst activity contributes significantly in the 0.1-10 keV energy range. We propose that the starburst activity strongly contributes to the far infrared luminosity of MKN 231; this is also suggested by the multiwavelength properties of MKN 231.

1. INTRODUCTION

MKN 231 is one of the best studied ULIRG and one of the most luminous object in the local universe. Although the nature of the primary energy source of ULIRGs (AGN vs. starburst activity) still remains rather enigmatic (see [4] and reference therein), in the case of MKN 231 optical and near infrared observations seem to suggest that a significant contribution to the infrared luminosity could be ascribed to AGN activity [7,9]. Moreover MKN 231 is also classified as a Broad

Absorption line (BAL) QSO [14]. On the other hand this galaxy is also undergoing an energetic starburst. This strong starburst activity combined with the luminous AGN makes MKN 231 one of the best example of the transition from starburst to AGN according to the scheme outlined in [13]. The presence of absorption possibly associated with the BAL outflows combined with the strong starburst activity, makes the X-ray continuum of MKN 231 particularly complex. ROSAT, ASCA and *Chandra* ([6,8,11,15]) observations have shown this complexity revealing both an extended soft X-ray emission (associated to the starburst activity) and a hard X-ray emission indicative of a heavily obscured AGN.

*This work has received financial support from ASI (I/R/037/01) and from ASI (I/R/062/02) under the project "Cosmologia Osservativa con XMM-Newton".

The models proposed to explain the flat X-ray spectra of MKN 231 accumulated so far (which were limited to $E < 10$ keV), invoke reprocessed emission: thus the estimate of the intrinsic power of the AGN can be obtained only through indirect arguments.

2. Observations and data reduction

MKN 231 was targeted by XMM-*Newton* on July 6th, 2001 and by *BeppoSAX* [1] from December 29th 2001 to January 1st 2002 (see Table 1). For the scientific analysis of the *BeppoSAX* observation only the data collected from the MECS and from the PDS have been considered. The XMM-*Newton* EPIC data have been filtered from high background time intervals and only events corresponding to pattern 0-12 for MOS and pattern 0-4 for pn have been used. In Fig. 1 the

Table 1
Exposure and count rates

Instrument	EXPOSURE ks	Cts/s 10^{-2}
pn	16	11 ± 1
MOS2	19.8	3.54 ± 0.14
MOS1	19.9	3.77 ± 0.14
PDS	76	6.58 ± 2.16
MECS	144	0.57 ± 0.02

XMM-*Newton* 0.5–2 keV (left panel) and the 4.5–10 keV (right panel) X-ray contours are overlaid to the optical DSS2-red image of MKN 231. The X-ray emission of MKN 231 appears to be extended in the low energy domain ($E < 2$ keV), while the hard (4.5–10.0 keV) X-ray brightness profile is comparable to the XMM-*Newton* point spread function (PSF).

3. The 0.5–50 keV spectrum.

The 0.5–50 keV spectrum of MKN 231 is particularly complex with both the signatures of the powerful starburst and of a heavily obscured AGN; a more detailed discussion of the spectral

modeling is reported in [2].

The 2–10 keV spectrum confirms that MKN 231 is characterized by: a weak Fe emission line ($EW \sim 300$ eV) and a very hard X-ray emission ($\Gamma \sim 0.8$ if a single power law (PL) model is fitted) with observed 2–10 keV luminosity of $\sim 5 \times 10^{42}$ erg s $^{-1}$. This latter is a factor 50 lower than what expected from the bolometric luminosity. All these observational evidences suggest that in the 2–10 keV bandpass we are seeing only reprocessed emission (through reflection or scattering on a Compton thick mirror).

The AGN emission (see Fig. 2) can be decomposed in:

- a transmitted PL which emerges above 10 keV (component a in Fig. 2) and is filtered by a high column density screen ($N_H \sim 2 \times 10^{24}$ cm $^{-2}$);
- a reprocessed (through scattering or reflection) PL continuum, which dominates the emission in the 2–10 keV range (component b). This reprocessed emission is also absorbed ($N_H \sim 10^{21} - 10^{22}$ cm $^{-2}$);
- a Fe K α emission line ($E_c = 6.39 \pm 0.15$ keV, $EW = 290 \pm 110$ eV; component d).

The 2–10 keV continuum and the weak Fe emission line could be explained with reflection from slightly ionized material or assuming that we see the AGN mainly through scattered emission (see [6] modeling of the *Chandra* data). In the latter scenario we assume that the Fe emission line is produced by transmission and is diluted from the scattered component.

It is worth noticing that, regardless of the possible models assumed for the hard X-ray emission (scattering or reflection), we always found a soft (0.5–2 keV) X-ray component associated with the starburst activity ($L_{(0.5-2)} = 6 - 9 \times 10^{41}$ erg s $^{-1}$). Furthermore in the proposed models another PL component is required to account for the 2–10 keV emission of MKN 231 ($L_{(2-10)} = 0.7 - 1.6 \times 10^{42}$ erg s $^{-1}$); this latter component could be identified with the hard X-ray emission from a population of High Mass X-ray binaries (component c

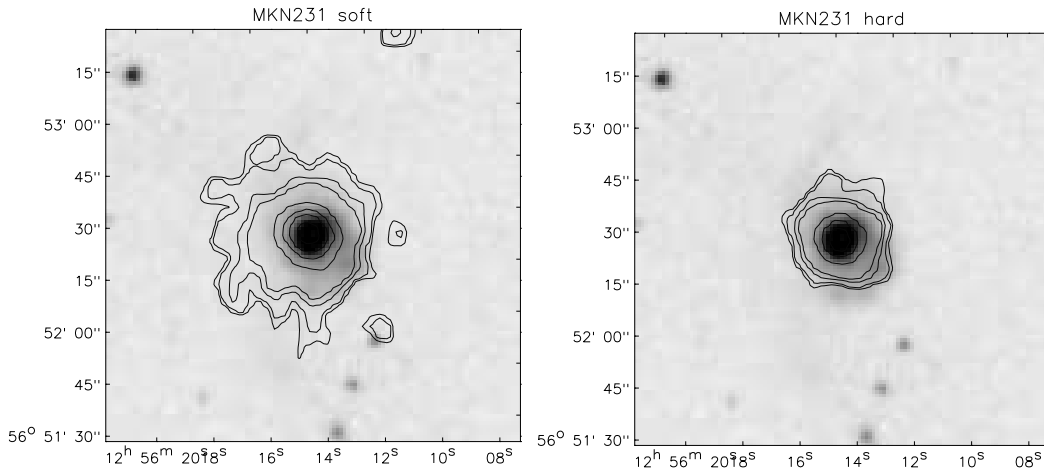


Figure 1. DSS2 image ($2' \times 2'$) of the field centered on MKN 231. Contours of the soft (0.5–2 keV; left panel) and hard (4.5–10 keV; right panel) X-ray emission have been overlaid on the optical image. The contours displayed correspond to 3σ , 4σ , 7σ , 10σ , 30σ , 50σ above the background.

in Fig. 2), which are expected to be copious in a strong starburst source like MKN 231.

4. Main Results

The main result reported here is that a highly absorbed ($N_H \sim 2 \times 10^{24} \text{ cm}^{-2}$) AGN component having an intrinsic 2–10 keV luminosity $1_{-0.5}^{+1.0} \times 10^{44} \text{ erg/s}$ has been detected (the error on this estimate refers to the range of luminosities derived with the two models considered). **This is the first direct measurement of the intrinsic power of the AGN hosted by MKN 231.**

This luminosity is about a factor 50 less than the infrared luminosity. Thus, the total FIR luminosity of the system cannot be entirely associated with the AGN, even assuming an AGN UV luminosity a factor 10 greater than the X-ray luminosity (as observed in QSOs; e.g. [3]). This suggests that the bulk FIR emission may be due to the starburst, in agreement with the results obtained modeling of the 1–1000 μm Spectral Energy Distribution [5].

These observations give also some suggestions on the physical status of the material surrounding the active nucleus in MKN 231. We identify the absorber which scatters or reflects the primary emission, with the BAL outflows which originate close to the central source. In particular the ionized mirror could be the inner part of this outflows (i.e. the “shielding gas” proposed by [6,12]). In both models proposed for the AGN emission, the scattered/reflected components are absorbed. This latter absorbing medium could be identified with the starburst regions (see e.g. [10]) or with a different line of sight through the BAL wind.

REFERENCES

1. G. Boella, R. C. Butler, G. C. Perola et al. 1997, A&AS, 122, 299
2. V. Braitto, R. Della Ceca, E. Piconcelli et al. A&A submitted
3. M. Elvis, B. J. Wilkes, J. C. McDowell, et al. 1994, ApJS, 95, 1

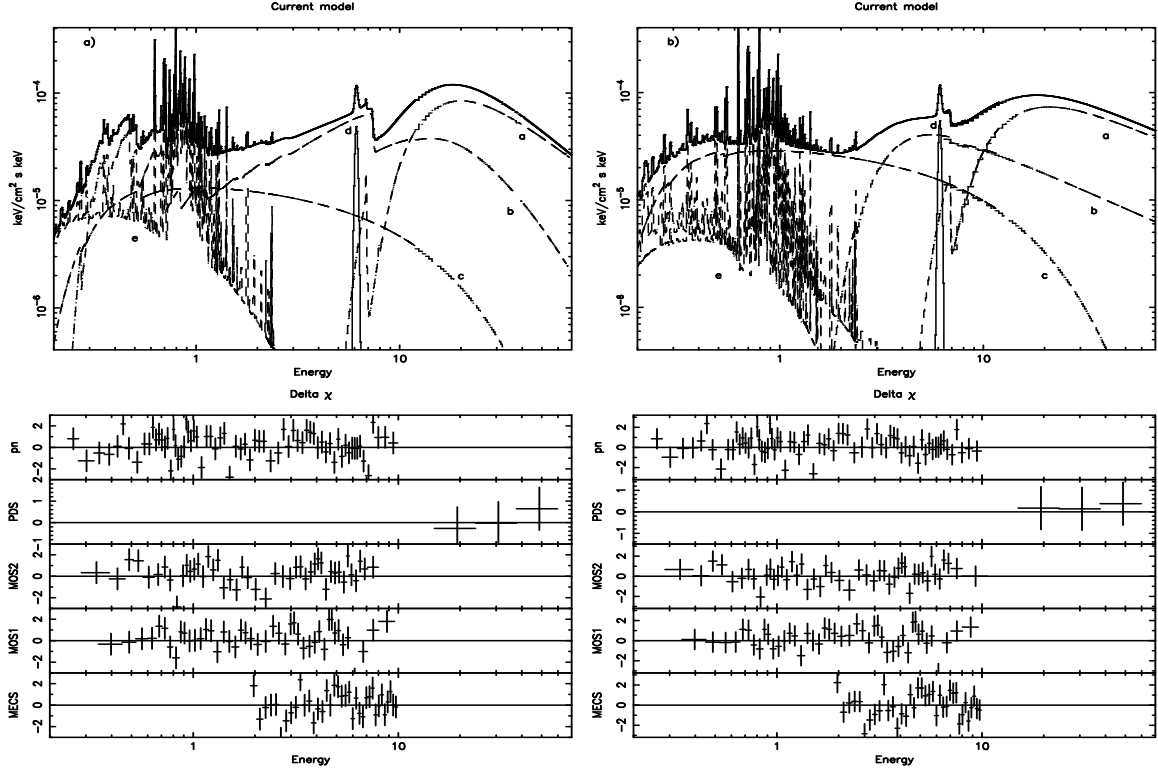


Figure 2. 0.2–50 keV data coverage. Upper panels: best fit models for the reflection-dominated (left panel) and scattering-dominated scenario (right panel). The spectral components are: a) a highly absorbed PL AGN; b) pure reflected AGN from slightly ionized material (left panel) or scattered AGN component (right panel); c) a cutoff PL associated with the binaries in the starburst; d) a narrow Gaussian line at 6.39 keV; and e) a thermal emission component associated with the starburst. Lower panels: residuals for the different detectors (from up to down: pn, PDS, MOS2, MOS1, MECS).

4. A. Franceschini, V. Braito, M. Persic et al. MNRAS in press (astro-ph/0304529)
5. D. Farrah, J. Afonso, A. Efstathiou et al. MNRAS in press astro-ph/0304154
6. S. C. Gallagher, W. N. Brandt, G. Chartas et al. 2002, ApJ, 569, 655
7. J. D. Goldader, & R. D. Joseph 1995, ApJ, 444, 97
8. K. Iwasawa 1999, MNRAS, 302, 96
9. A. Krabbe, L. Colina, N. Thatte, H. Kroker 1997, ApJ, 476, 98
10. N. A. Levenson, K. A. Weaver, T. M. Heckman, 2001, ApJ, 550, 230
11. P.R. Maloney & C. S.Reynolds 2000, ApJ, 545, 23
12. N. Murray, J. Chiang, S. A. Grossman, G. M. & Voit 1995, ApJ, 451, 498
13. D. B. Sanders & I. F. Mirabel 1996, ARA&A 34, 749
14. P. S. Smith, G. D. Schmidt, R. G. Allen, J. R. P. Angel 1995, ApJ, 444, 146
15. M. J. L. Turner 1999, ApJ, 511 142